

1 Technical note:

2 Optical properties of desert aerosol with non-spherical mineral particles: Data incorporated to OPAC

3

4 P. Koepke<sup>1</sup>, J. Gasteiger<sup>1</sup>, M. Hess<sup>2,3</sup>

5

6 [1] L-M-University Munich, Meteorological Institute, Theresienstr. 37, 80333 Muenchen, Germany

7 [2] DLR - German Aerospace Center, Remote Sensing Technology Institute, Oberpfaffenhofen,

8 82234 Weßling, Germany

9 [3] RASCIN, Thalkirchner Str. 284, 81371 Muenchen, Germany

10

11

12

13 Correspondence to P. Koepke (peter.koepke@lmu.de)

14

15

16 Abstract

17

18 Mineral particles in general are no spheres and assuming spherical particles, instead of more realistic  
19 shapes, has significant effects on modeled optical properties and so on the belonging remote sensing  
20 procedures for desert aerosol and the derived radiative forcing. Thus in a new version of the data  
21 base OPAC (Optical Properties of Aerosols and Clouds; Hess et al., 1998), the optical properties of the  
22 mineral particles are modeled describing the particles as spheroids with size dependent aspect ratio  
23 distributions, but with the size distributions and the spectral refractive indices not changed against  
24 the previous version of OPAC. The spheroid assumption is known to substantially improve the scatter-  
25 ing functions, but pays regard to the limited knowledge on particle shapes in an actual case. The rela-  
26 tive deviations of the optical properties of non-spherical mineral particles from those of spherical  
27 particles are for the phase function in in the solar spectral range up to +60% at scattering angles of  
28 about 130° and up to –60% in the backscatter region, but less than 2% for the asymmetry parameter.  
29 The deviations are generally small in the thermal infrared and for optical properties that are inde-  
30 pendent of the scattering angle. The improved version of OPAC (4.0) is freely available under

31 [www.rascin.net](http://www.rascin.net).

32

33

34 1. Introduction

35

36 The optical properties of aerosol particles are the basis for modeling their direct radiative forcing  
37 (Lacis a. Mishchenko, 1995; Haywood a. Boucher, 2000; Yi et al., 2011) and correspondingly for their  
38 effect on climate (McCormick a. Ludwig, 1967; Myhre et al., 2013). Moreover, the optical properties  
39 are necessary for all inversion techniques used for aerosol remote sensing (Koepke a. Quenzel, 1979;  
40 Kaufmann, 1993; Kalashnikova a. Sokolik, 2002; Nousiainen, 2009). Thus, for an easy availability of  
41 spectral optical properties of aerosol particles, the software package OPAC, Optical Properties of Aer-  
42 osols and Clouds, had been created (Hess et al., 1998).

43 The optical properties of aerosol particles in general are modeled using the size distribution and the  
44 spectral refractive indices of the particles. In the past, commonly the assumption has been made that  
45 the particles are spheres, using Mie-theory (Mie, 1908). This has different reasons: on the one hand,  
46 the assumption of spherical particles is reasonable in many cases, especially for water soluble aerosol  
47 types under typical meteorological conditions with relative humidity higher than 50%. On the other  
48 hand, the shape of individual particles is known only for a limited number of examples, because it  
49 needs electron microscopy measurements. Thus, for actual conditions, for practical use, the shape of  
50 particles, particularly as function of size, is not available. But even if the particle shape would be  
51 available, the problem remains that modeling of non-spherical particles is complex and time consum-

52 ing (Mishchenko et al., 2000; Kahnert, 2003). Thus the use of Mie-theory often is a good or the only  
53 possible assumption and it has also been used in OPAC.

54 Desert aerosol, besides sea salt, forms the largest fraction of the atmospheric particles (D’Almeida et  
55 al., 1991; Kinne et al., 2006). Thus desert aerosol is very important for the radiation budget and con-  
56 sequently for the climate, especially because it is distributed, often with high optical depth, over large  
57 areas. Since its amount shows very strong spatial and temporal variations (Sokolik et al., 2001), re-  
58 mote sensing methods are important for desert aerosol research. However, remote sensing is always  
59 based on the assumed particle characteristics.

60 Especially for mineral particles the optical properties modeled under the assumption of spherical  
61 shape are questionable, since these particles are generated by mechanical processes which give rise  
62 to highly irregular particle shapes, as to be seen by electron micrographs (Falkovich et al, 2001;  
63 Kandler et al., 2011).

64 In comparison to spherical particles the phase function of irregular particles generally shows in-  
65 creased sideward, but reduced backward scattering, if the particles are relatively large in comparison  
66 to the wavelength (Zerull et al., 1980; Koepke a. Hess, 1988; Nousiainen, 2009; and see Fig.1). Thus, if  
67 radiation data measured at short wavelengths are used to derive aerosol properties, the assumption  
68 of spheres may lead to wrong results. This holds also for particle properties derived from backscatter-  
69 lidar measurements (Gobbi et al., 2002; Wiegner et al., 2009; Sakai et al., 2014), since, amongst oth-  
70 ers, they are influenced by the lidar ratio, which combines backward scattering with the extinction  
71 coefficient. For passive remote sensing from satellite, an assumed wrong phase function of the parti-  
72 cles can introduce significant retrieval errors and for considerations of the radiation budget of mineral  
73 particles in the solar spectral range the assumption of spheres is a major source of error (Nousiainen,  
74 2009). The amount of solar radiation scattered back to a radiometer at a satellite depends on the  
75 scattering angle, i.e. the angles of Sun and satellite, on the aerosol optical thickness, and on the re-  
76 flectance at the ground. Thus the error in the case of assuming spherical particles is highly variable,  
77 and it is essential to use the appropriate scattering function (Horvath et al., 2006). The particle shape  
78 effect can cause up to 30% difference in dust forcing at the top of the atmosphere (Yi et al., 2011).

79

80 These aspects are the reason to account for the non-sphericity of mineral particles in OPAC (Hess et  
81 al., 1998) and so to improve this algorithm. The user-friendly data base and software package “Opti-  
82 cal Properties of Aerosol and Clouds” presents the single-scattering properties of 10 aerosol compo-  
83 nents that are given with size distribution and spectral refractive indices for a spectral range from  
84 ultraviolet to far-infrared. These components easily can be combined by the user to individual mix-  
85 tures, i.e. to variable aerosol types, for which phase functions and other optical and microphysical  
86 parameters are modeled after user request.

87 If a particle no longer is assumed to be spherical, the possible variability of the particle shape is in-  
88 creased dramatically, from spheres, over spheroids and cubes to really irregular particles (Cheng,  
89 1980). Thus, if the shape of particles will be taken into account for general modeling of the optical  
90 parameters, it is necessary to decide for simplifications. Moreover, a model is necessary that allows  
91 one to consider reasonable forms of non-spherical particles. In this paper the non-spherical mineral  
92 particles are approximated as spheroids, since this substantially improves the agreement between  
93 modelled and measured optical properties (Mishchenko et al., 1997; Kahnert et al., 2005) and an  
94 appropriate theory exists, the T-matrix method (Waterman, 1971).

95 In the new version of OPAC the optical properties of the mineral components are modeled as sphe-  
96 roids with the T-matrix method (Mishchenko a. Travis, 1998), with the aspect ratio distributions of  
97 the used spheroids varied with the particle size, as found by electron microscope investigations. The  
98 other microphysical properties of the components, the size distribution and the spectral refractive  
99 indices, have not been changed against the old OPAC. During the Saharan Mineral Dust Experiment  
100 field campaign (SAMUM-1), which was located close to the Sahara and its mineral sources and used a  
101 lot of different aerosol measurement systems (Heintzenberg, 2009), desert aerosol size distributions  
102 have been measured both in situ at an air plane (Weinzierl et al., 2009) and inferred by the AERONET  
103 network inversion algorithm from ground-based photometer measurements. The results differ con-

104 siderably (Müller et al., 2010), but the OPAC size distributions are in-between. Moreover, photometer  
105 measurements in the solar aureole (where the non-sphericity has no influence) and values modeled  
106 with OPAC type “desert” agree very well (Gasteiger, 2011). Also optical properties of Saharan dust  
107 measured by aircraft data in 1999 compare very favorably with OPAC results (Haywood et al., 2001)  
108 for radiative properties that are independent of the scattering angle, like asymmetry parameter, sin-  
109 gle scattering albedo and specific extinction coefficient, for which the non-sphericity has negligible  
110 influence. Thus the OPAC size distributions for desert aerosol are assumed to be adequate for a com-  
111 bination with the information on particle shape from SAMUM.  
112 Also not changed against the old OPAC is the possibility of the flexible mixing of the components and  
113 of the outcome of OPAC, like optical properties depending on relative humidity and available for a  
114 large wavelength range. In the new version of OPAC (4.0), which is freely available for non-  
115 commercial use, now the optical properties modeled for non-spherical mineral particles are taken  
116 into account, directly for practical application.

117

118

## 119 2. Methods

120

### 121 2.1. Non-spherical particle scattering

122

123 The most suitable method to model the optical properties of mineral aerosol particles on a systemat-  
124 ic basis (Wiegner et al., 2009) is the T-matrix method, TMM. It provides a solution of Maxwell’s equa-  
125 tions for the interaction of radiation with arbitrarily-shaped particles (Waterman, 1971) and is most  
126 efficient for rotationally symmetric particles. In our model the mineral particles are given as spher-  
127 oids, originating from rotation of ellipses about one of their axis. Thus, an additional microphysical  
128 parameter that has to be taken into account is the aspect ratio  $\epsilon$ , which is the ratio between the  
129 longest and the shortest axis (Dubovik et al., 2006). Moreover, the particles can be prolate (cigar like)  
130 and oblate (disk like) spheroids.

131 For the results in this paper and the new version of OPAC, the state-of-the-art TMM code from  
132 Mishchenko a. Travis (1998) for randomly oriented particles has been used for the mineral compo-  
133 nents. The T-matrix calculations are supplemented by geometric optics calculations with the code of  
134 Yang et al. (2007) for large particles not covered by the TMM code. Wiegner et al. (2009) show the  
135 size coverage of the TMM code, which can model dust spheroids up to size parameters,  $\chi=2\pi r/\lambda$ ,  
136 around 110 – 120 for aspect ratio 1.6 and smaller. For aspect ratio 3.0 the maximum size parameter  
137 of TMM is around 25. These codes have been used to create a data set of single particle scattering  
138 properties of spheroids covering a wide range of particle sizes, aspect ratios, and refractive indices.  
139 The grid of particle parameters in this data set is given in Gasteiger et al., 2011. The optical properties  
140 of the OPAC mineral components were calculated from this data set according to their microphysical  
141 properties described below. For the selection of the adequate aspect ratio distributions depending on  
142 particle size, measurements of the Saharan Mineral Dust Experiments (SAMUM I and SAMUM II) have  
143 been used (Kandler et al., 2009; Kandler et al., 2011).

144

145

### 146 2.2. Particle properties

147

148 This paper presents an improvement of OPAC, by modifying the shape of mineral particles. The other  
149 microphysical parameters used in OPAC, as the particle size distribution and the spectral refractive  
150 indices, have been left unchanged.

151 In OPAC the aerosol particles are given as components (Shettle a. Fenn, 1979; Deepak a. Gerber,  
152 1983) resulting from an internal mixture of particles of a certain origin. The particles of a component  $i$   
153 have a log-normal size distribution (Eq.1).

154

$$\frac{dN_i(r)}{dr} = \frac{N_i}{r \sqrt{2\pi} \log \sigma_i \ln 10} \exp\left(-\frac{1}{2} \left(\frac{\log r - \log r_{mod,i}}{\log \sigma_i}\right)^2\right) \quad (1)$$

156

157  $N_i$  is the total number of particles of the component  $i$  per cubic centimeter,  $r$  the particle radius,  $r_{mod,i}$   
 158 the mode radius of component  $i$  with respect to the particle number, and  $\sigma_i$  measures the width of  
 159 the distribution. The radius  $r$  of each spheroid is assumed to be the radius of a sphere with the orien-  
 160 tation-averaged geometric cross section of the spheroid. The relative optical properties do not de-  
 161 pend on  $N$ , thus they are given always for  $N=1$ . For absolute values of optical properties, for actual or  
 162 individual conditions,  $N_i$  must be chosen adequately for each component that will be taken into ac-  
 163 count.

164

165 The mineral dust is described in OPAC with three components as given in Tab. 1: Mineral Nucleation  
 166 Mode (MINM), Mineral Accumulation Mode (MIAM), and Mineral Coarse Mode (MICM), with  $r_{mod}$   
 167 and  $\sigma$  the data of the size distributions, and  $r_{min}$  and  $r_{max}$  the borders that have been taken into ac-  
 168 count for modeling the optical properties.

169

170 Tab. 1. Microphysical properties of mineral components

Component Mineral...		$r_{mod}$ [ $\mu\text{m}$ ]	$\sigma$	$r_{min}$ [ $\mu\text{m}$ ]	$r_{max}$ [ $\mu\text{m}$ ]
Nucleation mode	MINM	0.07	1.95	0.005	20
Accumulation mode	MIAM	0.39	2.00	0.005	20
Coarse mode	MICM	1.90	2.15	0.005	60

171

172 These mineral components can be mixed externally, also together with other components, to form  
 173 individual aerosol types. In general, both over deserts and for other aerosol conditions with a domi-  
 174 nant mass of mineral particles, also water-soluble particles (WASO) are present. These particles can  
 175 be assumed to be spherical. Their amount usually is small with respect to their mass per volume, but  
 176 since the particles are small their numbers per volume may be large.

177 In OPAC the aerosol type “desert” is a mixture of more than 200  $\mu\text{g}/\text{m}^3$  mineral particles and only 4  
 178  $\mu\text{g}/\text{m}^3$  water soluble particles (WASO), however, resulting in 2000 particles per  $\text{cm}^3$  of WASO, and 300  
 179  $\text{cm}^{-3}$  of mineral particles belonging to their three components. A small amount of WASO generally is  
 180 taken into account in the following results, which show optical properties of mixtures of mineral par-  
 181 ticles.

182 The refractive indices of the components are wavelength dependent (d Almeida et al., 1991; Koepke  
 183 et al., 1997). The particles of the mineral components all have the same refractive indices, since they  
 184 are assumed to result from the same sources at the surface. The refractive index is given with an im-  
 185 aginary part that is responsible for the absorption properties of the particles.

186

187 To describe the shape properties of mineral particles of different size, for each of the three mineral  
 188 components, the data of the “reference” case of SAMUM-1 have been used (Wiegner et al., 2009).  
 189 The reference case was a situation with a very homogeneous desert aerosol layer up to 5 km above  
 190 sea level which was very stable in time. The aspect ratio distribution of the particles was measured  
 191 using electron microscopy and is given depending on particle size intervals by Kandler et al. (2009).  
 192 For modeling the optical properties of mineral particles these wide aspect ratio distributions are ap-  
 193 plied, to account for the large variety of the natural dust particle shapes. The belonging modeling  
 194 results, compared to measured phase functions, are remarkably better than results when using only a  
 195 single aspect ratio (Mishchenko et al., 1997; Nousiainen a. Vermeulen, 2003). Moreover, all mineral  
 196 particles are assumed to be prolate, because this gives better agreement with measured scattering  
 197 matrix elements of dust particles than using oblate or mixtures of prolate and oblate spheroids  
 198 (Nousiainen a. Vermeulen, 2003).

199 It is worth mentioning that the aspect ratio distribution of mineral particles did not vary significantly  
 200 during SAMUM-1 and also not during the SAMUM-2 campaign, which was conducted further away

201 from the dust source Sahara (Kandler et al., 2009; Kandler et al., 2011). Thus the selected aspect ratio  
 202 distribution might be regarded as representative for Saharan dust.

203 The aspect ratio distributions depend on the size of the particles. For the reference case the relative  
 204 frequency of particles with a given aspect ratio is available for 6 ranges of particle size (Kandler et al,  
 205 2009; Wiegner et al., 2009). Some of them have similar aspect ratio distributions so that only three  
 206 radius ranges must be differentiated: For particles with  $r < 0.25 \mu\text{m}$  the frequency decreases strongly  
 207 with increasing aspect ratio. For particles with  $r > 0.5 \mu\text{m}$  the shape distributions for all analyzed size  
 208 intervals are similar with a small maximum for the aspect ratio of about 1.5. Between these two re-  
 209 gimes the particles between  $r = 0.25$  and  $r = 0.5 \mu\text{m}$  have an aspect ratio distribution that gives a  
 210 transition between the other two regimes (see Tab. 2).

211

212 Tab. 2. Aspect ratio distributions as function of particle radius interval according to Kandler et al.  
 213 (2009). The first line represents the range from  $\epsilon = 1.0$  to 1.3, the last line is valid for  $\epsilon > 2.9$  and the  
 214 other values cover  $\epsilon$ -intervals of 0.2.

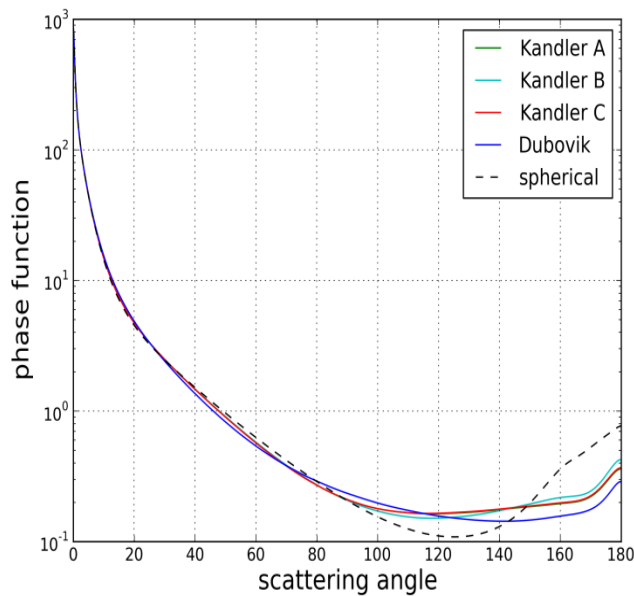
$\epsilon$	$r < 0.25 \mu\text{m}$	$0.25 \mu\text{m} < r < 0.5 \mu\text{m}$	$r > 0.5 \mu\text{m}$
1.2	0.535	0.225	0.103
1.4	0.289	0.212	0.234
1.6	0.108	0.156	0.218
1.8	0.040	0.110	0.157
2.0	0.015	0.075	0.101
2.2	0.007	0.054	0.065
2.4	0.003	0.039	0.041
2.6	0.001	0.028	0.027
2.8	0.001	0.022	0.018
3.0	0.001	0.079	0.036

215

216 Each OPAC mineral component contains particles in all radius ranges given in Tab. 2, with proportions  
 217 that are varying according to the size distribution of the components (Tab. 1). To check the shape  
 218 effects, as a first test (Kandler A) each mineral component is divided into the three radius ranges of  
 219 Tab. 2 and the belonging aspect ratio distribution of each range is applied. This test is the most exact  
 220 approach based on the available aspect ratio data. As a second test -- with respect of the idea of  
 221 OPAC to keep things easy -- for all particles of each of the three OPAC mineral components a fixed  
 222 aspect ratio distribution has been used: the distribution of  $r < 0.25 \mu\text{m}$  for MINM, of  $0.25 \mu\text{m} < r < 0.5$   
 223  $\mu\text{m}$  for MIAM, and of  $r > 0.5 \mu\text{m}$  for MICM (Kandler B). This test setup seems appropriate since the  
 224 mode radii of the three components (Tab.1) fall into these three radius intervals used to separate the  
 225 aspect ratio distributions (Tab.2). As a third test (Kandler C), the second test is modified by assuming  
 226 also for all particles of the accumulation mode (MIAM) the aspect ratio distribution that has been  
 227 measured for particles with  $r > 0.5 \mu\text{m}$ . This use of the aspect ratio distribution measured for the  
 228 larger particles also for MIAM was tested, since the maximum of the surface area distribution of  
 229 MIAM is close to a radius of  $1 \mu\text{m}$ . Finally a further association of radius and aspect ratio distribution  
 230 has been tested: Dubovik et al. (2006) has derived aspect ratio distributions by analyzing measured  
 231 phase functions, with the assumption that they are independent of the particle size. These are inves-  
 232 tigated as a forth test (Dubovik) for the particle shape effects.

233 As example for the different considerations of the aspect ratio distributions, in Fig.1 are shown the  
 234 phase functions under the assumption of spherical particles and for non-spherical particles after the  
 235 4 tested radius dependent aspect ratio distributions. The phase functions are given for a wavelength  
 236  $0.55 \mu\text{m}$  (however the results at other wavelengths are similar, see Fig.2), and as size distribution the  
 237 combination of the three mineral components of the aerosol type "desert" after OPAC, including  
 238 WASO at 0% relative humidity, has been used.

239



240  
241

242 Fig. 1. Phase functions at 0.55  $\mu\text{m}$  for the mixture of the mineral components after the aerosol type  
243 “desert”, under the assumption of spherical mineral particles and for mineral particles with various  
244 aspect ratio distributions (see text for details).

245

246 In Fig. 1 the increased sideward and reduced backward scattering clearly is to be seen which holds for  
247 all phase functions resulting from particles with non-spherical shape. The phase function after  
248 Dubovik is noticeably separated against those after Kandler A to C. But this result is not astonishing,  
249 since the direct electron microscopic investigations show that the aspect ratio distributions are size  
250 dependent, in contrast to the size-independent assumption by Dubovik. The phase functions after  
251 Kandler A (exact approach) and Kandler C are nearly identical, which means that the simpler assump-  
252 tions in Kandler C give already correct results. Thus for all optical property modeling of non-spherical  
253 mineral particles, both for the results shown in the following and for the new OPAC, the size depend-  
254 ent aspect ratio distribution after Kandler C is used.

255

256

### 257 3. Results

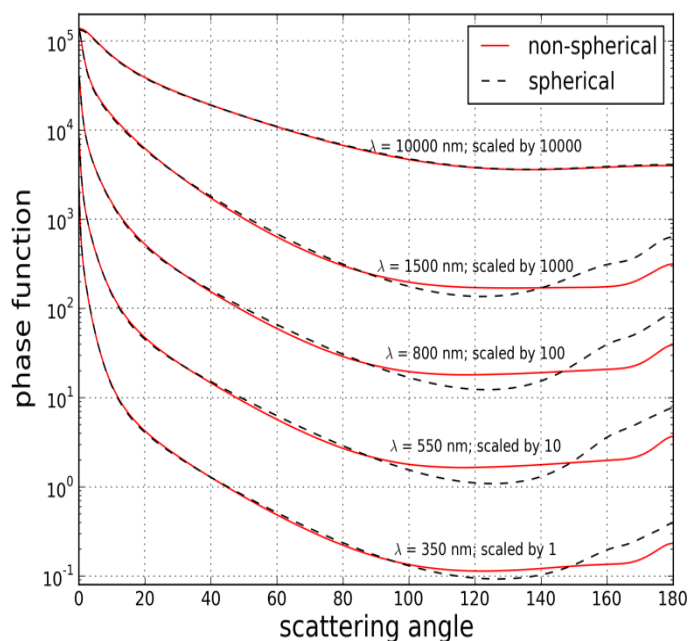
258

259 The effects of the particle shape are different for different optical properties, which is shown in this  
260 paragraph for a variation of the optical properties available from OPAC. Examples are presented for  
261 the deviations between optical properties caused by mineral particles that are assumed as spheres,  
262 on the one hand, and those assumed as spheroids with the aspect ratio distributions after Kandler C,  
263 on the other hand.

264

265 The phase function is very important for remote sensing of desert aerosol and for its radiative forcing,  
266 and moreover, as mentioned above, for this optical quantity the effect due to non-sphericity is large,  
267 especially in the solar spectral range.

268 Thus Fig. 2a shows the phase function for the two particle shape assumptions, for the mixture “de-  
269 sert” (Hess et al., 1998) and for different wavelengths. The assumed shape variation (spherical or  
270 non-spherical) is modeled only for the mineral particles: MINM 269.5  $\text{cm}^{-3}$ ; MIAM 30.5  $\text{cm}^{-3}$ , MICM  
271 0.142  $\text{cm}^{-3}$ . The 2000  $\text{cm}^{-3}$  particles of the WASO component always are assumed as spherical.

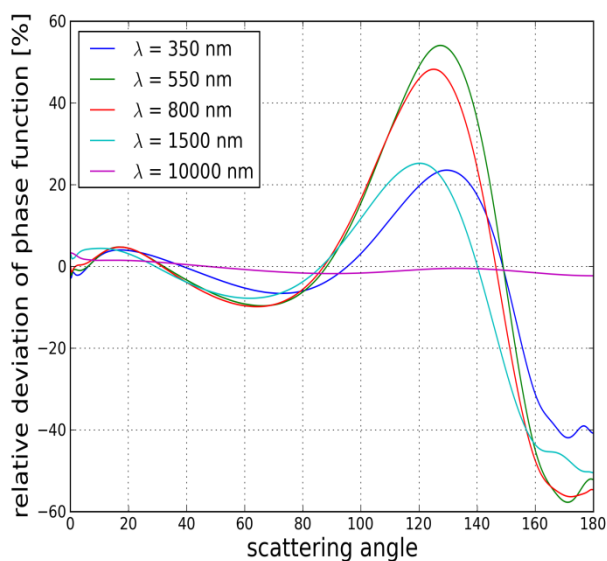


272  
273

274 Fig. 2a. Phase functions of desert aerosol for different wavelengths, assuming spherical and spheroidal mineral particles with a size dependent aspect ratio distribution after Kandler C. For details see  
275 text. The scale of the phase functions for the different wavelengths is shifted by a factor 10 in each  
276 case.  
277

278

279 The phase functions show the known strong forward peak of aerosol particles, which is not influ-  
280 enced by the particle shape. It is increasing with increasing size parameter, and thus decreasing with  
281 wavelength. The particle shape effect is clearly to be seen in Fig. 2a in the backward scattering region,  
282 but more pronounced in Fig. 2b, where the belonging percentage deviations between the phase func-  
283 tions for particles with size dependent aspect ratio distributions and for spherical particles are shown.  
284



285  
286

287 Fig. 2b. Relative deviations (%) of phase functions assuming spheroidal mineral particles from phase  
288 functions of spherical particles, for desert aerosol and the conditions shown in Fig. 2a.

289

290 The effect of the particle shape is up to almost + 60 % at scattering angles around 130° and – 60 %  
291 around 170°, in the backscatter region. The effect decreases with increasing wavelength and is nearly  
292 negligible at 10 μm, as also shown. The reason is that the shape properties of the particles become  
293 less relevant if the wavelength of the radiation becomes larger relative to the particle size. In contra-  
294 ry, the effect of the particle shape is relatively low at 350 nm, but this results from the strong absorp-  
295 tion of the mineral particles at this wavelength, which reduces the scattering effects in general and  
296 thus overcompensates the shape effect. As to be seen, the effect of the particle shape is strongest in  
297 the solar wavelength range, which is often used for aerosol remote sensing and which is essential for  
298 radiative forcing and thus for climate effects. This documents again the need to take the non-  
299 spherical shape of mineral particles into account for remote sensing or climate studies.

300 As mentioned, the aspect ratio distribution depends on the particle size. Thus size distributions with  
301 different amount of small and large particles may result in different variations of the phase function  
302 compared to that under the assumption of spheres. Since the life time of big particles in the atmos-  
303 phere is less than that of smaller particles, in a dust storm not only the total amount of mineral parti-  
304 cles in the air is high, but also the relative amount of large particles. During the transport, i.e. with  
305 the time after the dust generation, the particle amount will be reduced due to sedimentation, but  
306 this effect can be stronger for larger particles. Finally, for background conditions, the total amount of  
307 mineral particles is low, with the lowest amount of large particles (d'Almeida, 1987; Longtin et al.,  
308 1988; Tanré et al., 1988). The relative increasing amount of large particles with increasing turbidity  
309 that we assume to test the effect of non-sphericity with respect to particle size distribution is shown  
310 in Eqs. 2 – 4 (d'Almeida, 1987; Koepke et al., 1997). Given are correlations between the total number  
311 of mineral dust particles and the belonging numbers for the three mineral components.

312

$$313 \ln N_{MINM} = 0.104 + 0.963 \ln N_{\text{mineral}} \quad (2)$$

$$314 \ln N_{MIAM} = - 3.94 + 1.29 \ln N_{\text{mineral}} \quad (3)$$

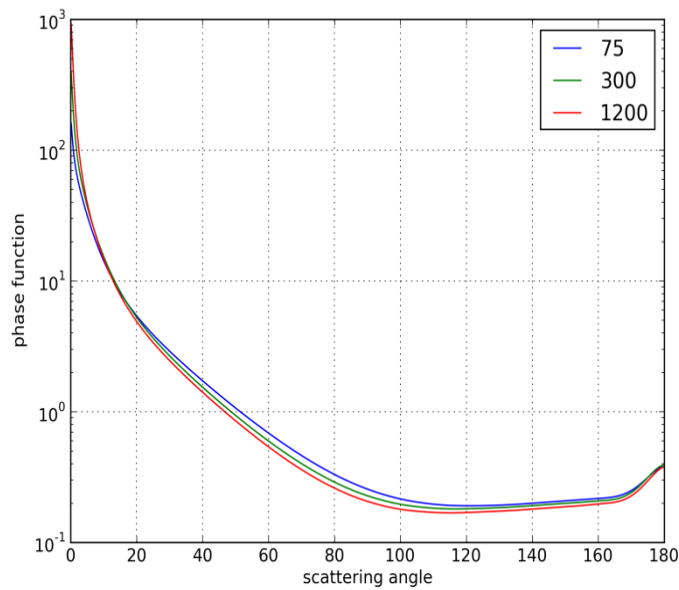
$$315 \ln N_{MICM} = - 13.7 + 2.06 \ln N_{\text{mineral}} \quad (4)$$

316

317 For desert aerosol with different turbidity, implemented with different total particle number and be-  
318 longing different number of particles of the three mineral components, in Fig. 3 the phase functions  
319 for non-spherical desert particles are shown. N gives the total number of mineral particles, the value  
320 of  $N_{\text{mineral}}$  in Eqs.2 - 4. N = 75 stands for “background desert” conditions, N=300 for average “desert”  
321 and N=1200 for “dust storm”. It can be seen that the general effect of the non-spherical particle  
322 shape is always given, but does not differ considerably for the different size distributions, as result of  
323 different total particle number. The effect of varying size distribution is more pronounced in the for-  
324 ward peak and the sideward scattering.

325





326  
327

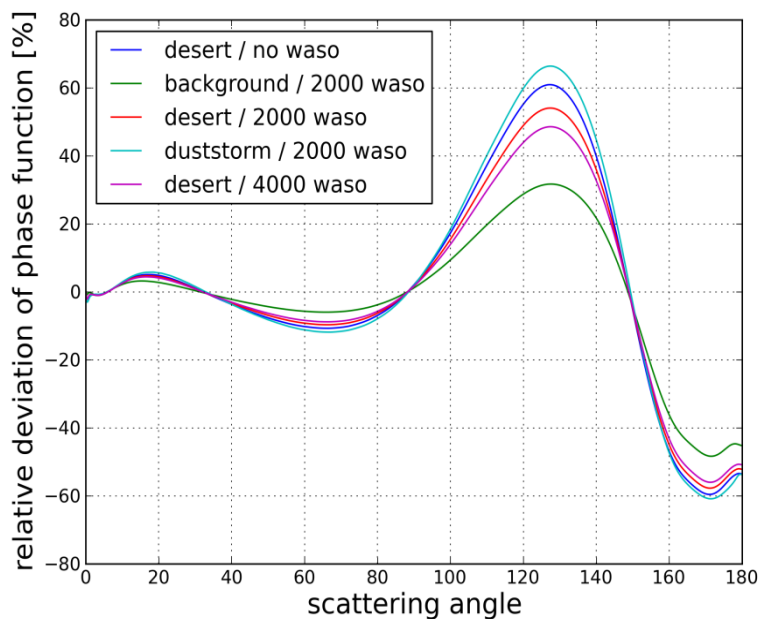
328 Fig. 3. Phase functions of desert aerosol at 0.8  $\mu\text{m}$ , with a mixture of the non-spherical mineral com-  
329 ponents MINM, MIAM and MICM after the Eqs. 2-4, using the total number of mineral particles given  
330 in the figure. In each case 2000 WASO particles assuming 0% r. h. are included.

331

332

333 As mentioned, the WASO particles are spheres, with the consequence that the variation of their  
334 amount changes the phase function of the mixture. This is shown in Fig. 4 for “desert” with different  
335 amount of WASO, on the one hand, and for average amount of 2000 WASO particles, but in combina-  
336 tion with mineral particles for “background” and for “dust storm” conditions, on the other hand.

337



338

339

340 Fig. 4. Relative deviations (%) of phase functions at 0.55  $\mu\text{m}$ , assuming spheroidal mineral particles,  
341 from phase functions of spherical particles, for different combinations of the components WASO,  
342 MINM, MIAM and MICM (for details see text).

343

344 Figure 4 shows that the effects due to the particle shape increase from background over desert to  
345 dust storm if the number of WASO is fixed, simply due to the increasing amount of non-spherical  
346 mineral particles. In contrary, the effect due to non-spherical shape is reduced, to be seen for the  
347 type “desert”, if the amount of spherical WASO particles is increased. But it should be mentioned that  
348 the effect due to doubling or omitting WASO for the relative deviations of the phase function is less  
349 than the effect due to the variation of the amount of the mineral particles.

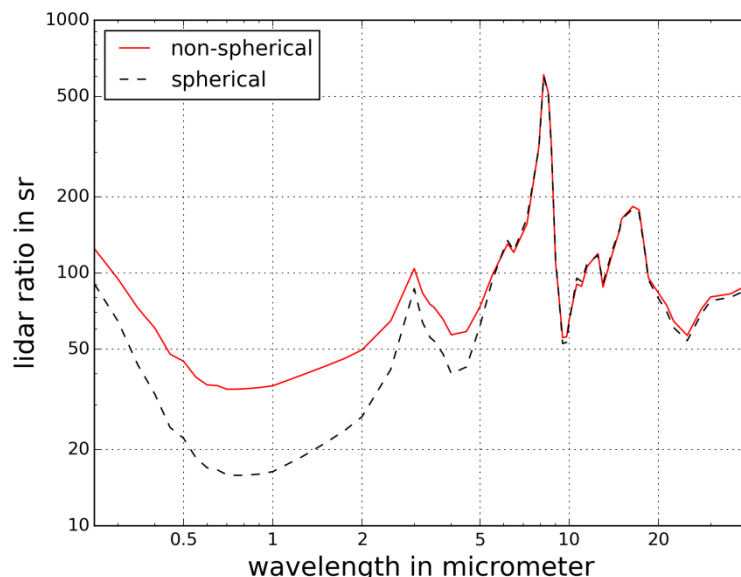
350

351 For the determination of the height dependent aerosol extinction coefficients, often backscatter lidar  
352 systems or ceilometers are used, because they are cheaper than higher sophisticated lidar instru-  
353 ments (Mona et al., 2012; Wiegner et al., 2014). However, for these instruments the measured signal  
354 is result of both the extinction coefficient and the phase function at  $180^\circ$ . Thus, to get the interesting  
355 height dependent extinction coefficient, it is necessary to use a quantity “lidar ratio”, which depends  
356 on the phase function and thus on the particle shape.

357 Fig. 5 shows the lidar ratio for the aerosol type “desert”, both under the assumption of non-spherical  
358 and spherical mineral particles. The values are given for a wavelength range up to  $40 \mu\text{m}$ , although no  
359 lidar instruments are available for wavelength larger  $\approx 2 \mu\text{m}$ . Moreover for the large wavelengths, the  
360 particles behave more and more like spheres, as already to be seen in Fig. 2b. For the interesting  
361 wavelength range around and below  $1 \mu\text{m}$ , however, the consideration of non-sphericity is essential.  
362 With respect to independently measured lidar ratios, the agreement with modeled values is much  
363 better under the assumption of spheroids than of spheres (Gobbi et al., 2002). The lidar ratios to be  
364 seen in Fig. 4 are in good agreement with measured values from SAMUM (Groß et al., 2011). This also  
365 generally is valid for all lidar-wavelengths that have been used during SAMUM, but here the agree-  
366 ment between measured and modeled lidar ratios was reduced for  $355 \text{ nm}$ , probably due to wrong  
367 assumptions with respect to the refractive index (Wiegner et al., 2009).

368

369



370

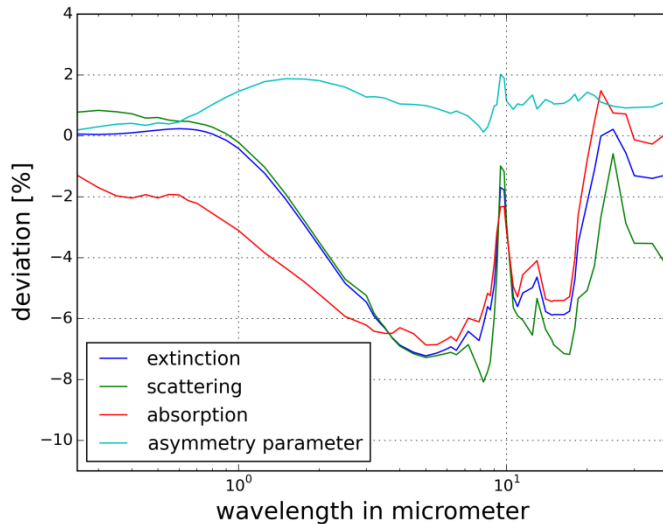
371 Fig. 5. Modeled values of the lidar ratio for “desert” aerosol under the assumption of spherical and  
372 non-spherical particles.

373

374

375 Optical quantities that are independent of the scattering angle or given as ratio between wavelengths  
376 are expected to be less sensitive with respect to the particle shape. To investigate this aspect, in Fig. 6  
377 relative differences between spherical and non-spherical desert particles are presented for the spec-  
378 tral scattering -, absorption - and extinction- coefficients and for the asymmetry parameter. For all

379 these quantities the deviations are less than 6 % and even less than 4 % in the part of the solar spec-  
 380 trum that is most relevant for climate effects. The same low dependency on the particle shape also  
 381 holds for the single scattering albedo and the Ångstrom coefficient, not shown in a figure.  
 382



383  
 384

385 Fig.6. Deviation (%), between spherical and non-spherical “desert” aerosol for different optical quan-  
 386 tities

387  
 388  
 389

390 4. New version: OPAC (4.0)

391

392 The main improvement of the new version of OPAC is the consideration of the non-sphericity of min-  
 393 eral particles. In OPAC always the large wavelength range between 0.25 and 40 μm is considered,  
 394 with the consequence that the improved particle shape of mineral particles works both in the solar  
 395 and in the infrared spectral region. Additionally new in OPAC (4.0) is the possibility to model the par-  
 396 ticle mass for different cut off radii, as used e.g. for PM10. On the other hand, the component “min-  
 397 eral transported”, MITR, no longer is considered. This component had been used to describe desert  
 398 aerosol under very remote conditions, as part of aerosol in polar regions. However, the amount of  
 399 mineral dust particles should be reduced continuously on its way from the source, depending on their  
 400 life time. This is possible with the remaining mineral components (e.g. using Eqs. 2-4), instead of  
 401 switching to MITR. Thus the aerosol type “Antarctic” in OPAC has been modified.

402 As discussed in the paper, the shape of the mineral particles has been improved. To avoid mistakes,  
 403 the new mineral components are named in the new OPAC version with an N at the end, standing for  
 404 non-spherical. The change from spheres to spheroids was made on the basis of cross section equiva-  
 405 lence, resulting in a small reduction of the particle volume and thus the particle mass, resulting in the  
 406 reduction factors shown in Tab. 3.

407

408 Tab. 3. Reduction factors for particle volume and mass for the non-spherical mineral components,  
 409 compared to the old components.

MINM → MINN	0.9754
MIAM → MIAN	0.9273
MICM → MICN	0.9273

410

411 All the other microphysical aerosol properties are unchanged against the previous version of OPAC.  
412 Also the new version of OPAC gives the possibility to combine different aerosol components, in each  
413 case with individually decided particle number density for each component.  
414 Results of OPAC (4.0) are a large number of optical properties (like phase function, scattering- absorp-  
415 tion- and extinction coefficient, asymmetry parameter, single scattering albedo, Ångstrom coefficient,  
416 lidar ratio and visibility)and particle mass per volume. All properties can be modeled for different  
417 relative humidity and the optical properties are available as spectral values for the wide wavelength  
418 range of 0.25 to 40  $\mu\text{m}$  and spectrally weighted for the solar and terrestrial range. For non-  
419 commercial use OPAC (4.0) is freely available: [www.rascin.net](http://www.rascin.net).

420

421

## 422 5. Conclusion

423

424 Aerosol particles are one of the main gaps in the present knowledge of radiative forcing (Myhre et al.,  
425 2013), and mineral particles are especially essential due to their large amount and temporal and spa-  
426 tial variability. Since mineral particles in general are no spheres, Mie-theory may lead to wrong val-  
427 ues, both, if their optical properties are modelled based on size distribution and refractive index, and  
428 vice versa, if remote sensing data are used to get aerosol properties. Thus, the optical properties of  
429 mineral particles in the new version of OPAC are derived using T-Matrix method for spheroids. As  
430 described in this paper the non-sphericity is given by typical size dependent aspect ratio distributions  
431 of spheroids, which have been derived from measurements at observation campaigns. The prede-  
432 fined components in OPAC, now also for non-spherical mineral particles, are a big convenience, be-  
433 cause users do not need to decide for individual single particle properties, as available from various  
434 studies and data bases (Nousiainen, 2009; Meng et al., 2010).

435 The differences between spherical and non-spherical mineral particles are shown for a wide range of  
436 optical properties of desert aerosols. They are small, nearly negligible, for angular-independent opti-  
437 cal quantities, like extinction-, scattering- and absorption- coefficient, asymmetry factor, single scat-  
438 tering albedo and Ångstrom coefficient. However the differences between spherical and non-  
439 spherical particles are large, up to 60 %, in the sideward and backward scattering regions of the phase  
440 functions in the solar spectral range. As a consequence the deviations also are large in the lidar ratio,  
441 a parameter required to get height dependent extinction values from often used backscatter lidar  
442 measurements. The effect of the particle shape decreases with wavelength, since for wavelengths  
443 that are rather large with respect to the particle size, the irregular particle shape is of less relevance.  
444 It should be born in mind that the size distribution and the complex refractive index of the aerosol  
445 particles are very important for their optical properties. For the radiative properties in the thermal  
446 infrared the uncertainty in the refractive index will outperform the shape effect, which moreover  
447 depends on the absorption of the particles (Legrand et al., 2014). However, in this article only the  
448 aspect of the shape of mineral particle is discussed, and in the new version of OPAC the shape of the  
449 mineral particles has been improved, but the assumed size distributions and spectral refractive indi-  
450 ces have not been changed. This will be done in the future, where it is planned also to add a stronger  
451 absorbing mineral component that allows for a larger variability of mixtures to describe desert aero-  
452 sol.

453 Since the solar spectral range is often used for remote sensing of aerosol particles, on the one hand,  
454 and relevant for aerosol radiative forcing, on the other hand, the consideration of the phase functions  
455 of non-spherical mineral particles is a real improvement of OPAC, now available as version 4.0.

456

## 457 Acknowledgements

458 This publication was partly funded by LMU Munich's Institutional Strategy LMUexcellent within the  
459 framework of the German Excellence Initiative.

460

461

## 462 References

463  
464 d 'Almeida, G.A.: On the variability of desert aerosol radiative characteristics, *J. Geophys. Res.*, 92, D3,  
465 3017 – 3026, 1987.

466 d 'Almeida, G.A., Koepke, P., and Shettle, E.P.: Atmospheric aerosols, A. Deepak Publ. Hampton, Vir-  
467 ginia, USA, pp 561, 1991.

468 Cheng, R.J.: Physical properties of atmospheric particulates , In: *Light scattering by irregularly shaped*  
469 *particles* [D.W. Schuerman (ed.)], Plenum Press, New York, USA, 69 - 78, 1980.

470 Deepak, A. and Gerber, H.E.: Report of the experts meeting on aerosols and their climatic effects,  
471 WCP-55, World Meteorolog. Org., Geneva, Switzerland, 107 pp, 1983.

472 Dubovik, O., Sinyuk, A., Lapyonok,T., Holben, B.N., Mishchenko, M.I., Yang, P., Eck, T.F., Volten, H.,  
473 Munoz, O., Veihelmann, B., van der Zande, W.J., Leon, J.F., Sorokin, M.,and Slutsker, I.: Appli-  
474 cation of spheroid models to account for aerosol particle non-sphericity in remote sensing of  
475 desert dust, *J. Geophys. Res.- Atmos.*, 111, D11208, 1 - 34, 2006

476 Falkovich, A.H., Gomez, E., Lewin, Z., Formenti, P., and Rudich, Y.: Analysis of individual dust particles,  
477 *J. Geophys. Res. – Atmos.*, 106 ,D16, 18029 – 18036, 2001.

478 Gasteiger, J.K. : Retrieval of microphysical properties of desert dust and volcanic ash aeosols from  
479 ground –based remote sensing, Diss. Univ. Muenchen, 124 pp., 2011.

480 Gasteiger, J., Groß, S., Freudenthaler, V., and Wiegner, M.: Volcanic ash from Iceland over Munich:  
481 mass concentration retrieved from ground-based remote sensing measurements, *Atmos.*  
482 *Chem. Phys.*, 11, 2209-2223, 2011.

483 Gobbi, G.P., Barnaba, F., Blumthaler, M., Labow, G., and Herman, J.R.: Observed effects of particles  
484 non-sphericity on the retrieval of marine and desert dust aerosol optical depth by lidar,  
485 *Atmos. Res.*, 61, 1 – 14, 2002.

486 Groß, S., Tesche, M., Freudenthaler, V., Toledano, C., Wiegner, M., Ansmann, A., Althausen, D., and  
487 Seefeldner, M.: Characterization of Saharan dust, marine aerosols and mixtures of biomass-  
488 burning aerosols and dust by means of multi-wavelength depolarization and Raman lidar  
489 measurements during SAMUM 2, *Tellus B*, 63, 706-724, 2011.

490 Haywood, J.M. and Boucher, O.: Estimates of direct and indirect radiative forcing due to tropospheric  
491 aerosol: A review, *Rev. Geophys.*, 38, 513 – 543, 2000.

492 Haywood, J.M., Francis, P.N., Glew, M.D., and Taylor, J.P.: Optical properties and direct radiative effect  
493 of Saharan dust: A case study of two Saharan dust outbreaks using aircraft data, *J. Geophys.*  
494 *Res.- Atmos.*, 106, D16, 18417 – 18430., 2001

495 Heintzenberg, J. :The SAMUM-1 experiment over Southern Morocco: overview and introduction,  
496 *Tellus B*, 61, 2 – 11, 2009.

497 Hess, M., Koepke, P., and Schult, I.: Optical properties of aerosols and clouds: The software package  
498 OPAC, *Bul. Am. Meteorol. Soc.*, 79, 5, 831 – 844, 1998.

499 Horvath, H., Kasahara, M., Tohno, S., and Kocifaj, M.: Angular scattering of the Gobi desert aerosol  
500 and its influence on radiative forcing, *J. Aerosol Sci.*, 37, 1287 – 1302, 2006.

501 Kalashnikova, O.V. and Sokolik, I.N.: Importance of shapes and compositions of wind-blown dust par-  
502 ticles for remote sensing at solar wavelengths, *Geophys. Res. Lett.*, 29, 10, 38-1 – 38-4, 2002

503 Kahnert, F.M.: Numerical methods in electromagnetic scattering theory, *J. Quant. Spectrosc. Rad.*  
504 *Transfer*, 79, 775 – 824, 2003.

505 Kahnert, M., Nousiainen, T., and Veihelmann, B.: Spherical and spheroidal model particles as an error  
506 source in aerosol climate forcing and radiance computations: A case study for feldspar aero-  
507 sols, *J. Geophys. Res.-Atmos.*, 110, D18S13, 2005.

508 Kandler, K., Schütz, L., Deutscher, C., Ebert, M., Hofmann, H., Jäckel, S., Jaenicke, R., Knippertz, P.,  
509 Lieke, K., Massling, A., Petzold, A., Schladitz, A., Weinzierl, B., Wiedensohler, A., Zorn, S., and  
510 Weinbruch, S.: Size distributions, mass concentrations, chemical and mineralogical composi-  
511 tion, and derived optical parameters of the boundary layer aerosol at Tinfou, Morocco, during  
512 SAMUM 2006, *Tellus B*, 61, 32 – 50, 2009.

513 Kandler, K., Lieke, K., Benker, N., Emmel, C., Küpper, M., Müller-Ebert, D., Scheuvsens, D., Schladitz, A.,  
514 Schütz, L., and Weinbruch, S. : Electron microscopy of particles collected at Praia, Cap Verde,

515 during the Saharan mineral dust experiment: particle chemistry, shape, mixing state and  
516 complex refractive indices, *Tellus B*, 63, 457–496, 2011.

517 Kaufmann, Y.J.: Measurements of the optical thickness and the path radiance - Implications on aero-  
518 sol remote sensing and atmospheric corrections, *J. Geophys. Res.*, 98, 2677 – 2692, 1993.

519 Kinne, S., Schulz, M., Textor, C., Guibert, S., Balkanski, Y., Bauer, S.E., Berntsen, T., Berglen, T.F., Bou-  
520 cher, O., Chin, M., Collins, W., Dentener, F., Diehl, T., Easter, R., Feichter, J., Fillmore, D., Chan,  
521 S., Ginoux, P., Gong, S., Grini, A., Hendricks, J., Herzog, M., Horowitz, L., Isaksen, I., Iversen, T.,  
522 Kirkevåg, A., Kloster Koch, D., Kristjansson, J.E.R., Krol, M., Lauer, A., Lamarque, J.F., Lesins, G.,  
523 Liu, X., Lohmann, U., Montanaro, V., Myhre, C., Penner, J., Pitari, G., Reddy, S., Seland, O.,  
524 Stier, P., Takemura, T., and Tie, X.: An AeroCom initial assessment – optical properties in aero-  
525 sol component modules of global models, *Atmos. Chem. Phys.*, 6, 1815 – 1834, 2006.

526 Koepke, P. and Quenzel, H.: Turbidity of the atmosphere determined from satellite, *J. Geophys. Res.*,  
527 84, C12, 7847 – 7856, 1979.

528 Koepke, P. and Hess, M.: Scattering functions of tropospheric aerosols: the effects of non-spherical  
529 particles, *Appl. Optics*, 27, 12, 2422 – 2430, 1988.

530 Koepke, P., Hess, I., Schult, and Shettle, E.P.: Global Aerosol Data Set, Report No.243, MPI Hamburg,  
531 Germany, 44 pgs, 1997.

532 Lacis, A.A. and Mishchenko, M.I.: Climate forcing, climate sensitivity, and climate response: a radiative  
533 modeling perspective on atmospheric aerosols. In: *Aerosol forcing of climate* [Charlson, R.J.  
534 and Heintzenberg, J. (eds.)] John Wiley & Sons, 11 – 42, 1995.

535 Legrand, M., Dubovik, O., Lapyonok, T., and Derimian, Y.: Accounting for particle non-sphericity in  
536 modeling mineral dust radiative properties in the thermal infrared. *J. Quant. Spectroscop.*  
537 *Rad. Transfer*, 149, 219 – 240, 2014.

538 Longtin, D.R., Shettle, E.P., Hummel, J.R., and Pryce, J.D.: A desert aerosol model for radiative transfer  
539 studies, In: *Aerosols and climate* [Hobbs, P.V. and McCormick, M.P. (eds.)]A. Deepak Publ.,  
540 Hampton Virginia, USA, 261 – 269, 1988.

541 McCormick, R.A. and Ludwig, J.H.: Climate modification by atmospheric aerosols, *Science*, 156, 1358  
542 – 1359, 1967.

543 Meng, Z., Yang, P., Kattawar, G.W., Bi, L., Liou, K.N., and Laszlo, I.: Single-scattering properties of tri-  
544 axial ellipsoidal mineral dust aerosols: A database for application to radiative transfer calcula-  
545 tions, *J. Aerosol Sci.*, 41, 501 – 512, 2010.

546 Mie, G.: Beiträge zur Optik trüber Medien, speziell kolloidaler Metallösungen, *Ann. Physik*, 25, 377 –  
547 445, 1908.

548 Mishchenko, M.I., Travis, L.D., Kahn, R.A., and West, R.A.: Modeling phase functions for dust-like  
549 tropospheric aerosols using a shape mixture of randomly oriented polydisperse spheroids, *J.*  
550 *Geophys. Res.*, 102, 13543 – 13553, 1997.

551 Mishchenko, M.I. and Travis, L.D.: Capabilities and limitations of a current Fortran implementation of  
552 the T-Matrix method for randomly oriented, rotationally symmetric scatterers, *J. Quant.*  
553 *Spectrosc. Rad. Transfer*, 60, 309 – 324, 1998.

554 Mishchenko, M.I., Hovenier, J.W., and Travis, L.D. (Eds): *Light scattering by nonspherical particles:*  
555 *Theory, measurements, and applications*, Academic Press, San Diego, USA, 2000.

556 Mona, L., Liu, Z., Müller, D., Omar, A., Papayannis, A., Pappalardo, G., Sugimoto, N., and Vaughan, M.:  
557 Lidar measurements for desert dust characterization: An Overview, *Adv. Meteorology*, 2012,  
558 ID356265, 36 pp, 2012.

559 Müller, D., Weinzierl, B., Petzold, A., Kandler, K., Ansmann, A., Müller, T., Tesche, M., Freudenthaler, V.,  
560 Esselborn, M., Heese, B., Althausen, D., Schaditz, A., Otto, S., and Knippertz, P.: Mineral dust  
561 observed with AERONET Sun photometer, Raman lidar, and in situ instruments during  
562 SAMUM 2006: Shape-independent particle properties, *J. Geophys. Res.- Atmos.*, 115,  
563 D07202, 2010.

564 Myhre, G., Shindell, D., Bréon, F.-M., Collins, W., Fuglestedt, J., Huang, J., Koch, D., Lamarque, J.-F.,  
565 Lee, D., Mendoza, B., Nakajima, T., Robock, A., Stephens, G., Takemura, T., and Zhanh, H.: An-  
566 thropogenic and natural radiative forcing, In: *Climate Change 2013* [Stocker, T.F., Qin, D.,

567 Plattner, G.-K., Tignor, M., Allen, S.K., Boschung, J., Nauels, A., Xia, Y., Bex, V., and Midgley,  
568 P.M. (eds.)] Cambridge Univ. Press, Cambridge, UK, and New York, USA, 2013.

569 Nousiainen, T. and Vermeulen, K.: Comparison of measured single-scattering matrix of feldspar with  
570 T-matrix simulations using spheroids, *J. Quant. Spec. Rad. Trans.*, 79, 1031 – 1042, 2003.

571 Nousiainen, T. : Optical modeling of mineral dust particles: A review, *J. Quant. Spectroscop. Ra.*, 110,  
572 1261 – 1279, 2009.

573 Sakai ,T., Orikasa, N., Nagai, T., Murakami, M., Tajiri, T., Saito, A., Yamashita, K., and Hashimoto, A.:  
574 Balloon-borne and Raman lidar observations of Asian dust and cirrus cloud properties over  
575 Tsukuba, Japan, *J. Geophys. Res.- Atm.*, 119, 6, 3295 – 3308, 2014.

576 Shettle, E.P. and Fenn, R.W.: Models for the aerosols of the lower atmosphere and the effects of hu-  
577 midity variations on their optical properties, Report AFGL-TR-79-0214, AFGL, Hanscom AFB,  
578 Mass, USA, pp.94, 1979.

579 Sokolik, I.N., Winker, D.M., Bergametti, G., Gilette, D.A., Carmichel, G., Kaufmann, Y.J., Gomes, L.,  
580 Schmetz, I., and Penner, J.E.: Introduction to special section: outstanding problems in quanti-  
581 fying the radiative impacts of mineral dust, *J. Geophys. Res. –Atmos.*, 106, D16, 18015 –  
582 18027, 2001.

583 Tanré, D., Devaux, C., Herman, M., and Santer, R.: Radiative properties of desert aerosols by optical  
584 ground-based measurements at solar wavelengths, *J. Geophys. Res. – Atmos.*, 93, D11, 14223  
585 – 14231, 1988.

586 Waterman, P.: Symmetry, unitarity, and geometry in electromagnetic scattering, *Phys. Rev.*, D4, 825 –  
587 839, 1971.

588 Weinzierl, B., Petzold, A., Esselborn, M., Wirth, M., Rasp, K., Kandler, K., Schütz, L., Koepke, P., and  
589 Fiebig, M. : Airborne measurements of dust layer properties, particle size distribution and  
590 mixing state of Saharan dust during SAMUM 2006, *Tellus B*, 61, 96-117, 2009.

591 Wiegner, M., Gasteiger, J., Kandler, K., Weinzierl, B., Rasp, K., Esselborn, M., Freudenthaler, V., Heese,  
592 B., Toledano, C., Tesche, M., and Althausen, D.: Numerical simulations of optical properties of  
593 Saharan dust aerosols with emphasis on lidar applications, *Tellus B*, 61, 180 – 194. 2009.

594 Wiegner, M., Madonna, F., Biniotoglou, I., Forkel, R., Gasteiger, J., Geiß, A., Pappalardo, G., Schäfer, K.,  
595 and Thomas, W.: What is the benefit of ceilometers for aerosol remote sensing? *Atmos.*  
596 *Meas. Tech.* 7, 1979 – 1997, 2014.

597 Yang, P., Feng, Q., Hong, G., Kattawar, G.W., Wiscombe, W.J., Mishchenko, M.I., Dubovik, O., Laszlo, I.,  
598 and Sokolik, I.N.: Modeling of the scattering and radiative properties of nonspherical dust-like  
599 aerosols, *J. Aerosol Sci.*, 38, 995-1014, 2007.

600 Yi, B., Hsu, C.N., Yang, P., and Tsay, S.-C.: Radiative transfer simulation of dust-like aerosols: Uncertain-  
601 ties from particle shape and refractive index, *J. Aerosol Sci.*, 42, 631 – 644, 2011.

602 Zerull, R.H., Giese, R.H., Schwill, S., and Weiss, K.: Scattering by particles of nonspherical shape, In:  
603 *Light scattering by irregularly shaped particles* [Schuerman, D.W. (ed.)], Plenum Press, New  
604 York, USA, 273 – 282, 1980.

605

606